LBL-27582

Lawrence Berkeley Laboratory
UNIVERSITY OF CALIFORNIA

Presented at the Joint Meeting of the American Physical Society and the American Association for the Advancement of Science, Biological Physics Section, San Francisco, CA, January 14–21, 1989

Damage and Repair of Irradiated Mammalian Brain

K. Frankel, E. Lo, M. Phillips, J. Fabrikant, K. Brennan, P. Valk, A. Poljak, R. Delapaz, and K. Woodruff

July 1989

Donner Laboratory

Biology & Medicine Division

Prepared for the U.S. Department of Energy under Contract Number DE-AC03-76SF00098.

DISCLAIMER

Damage and Repair of Irradiated Mammalian Brain †

K. Frankel, E. Lo, M. Phillips, J. Fabrikant, K. Brennan, P. Valk,
Research Medicine and Radiation Biophysics,
Lawrence Berkeley Laboratory

A. Poljak, R. Delapaz, Stanford University Medical Center

K. Woodruff, Brookside Hospital

Presented at the Joint Meeting of the American Physical Society and the American Association for the Advancement of Science, Biological Physics Section, San Fransisco, CA, 14-21 January 1989.

ABSTRACT

We have demonstrated that focal charged particle irradiation of the rabbit brain can create well-defined lesions which are observable by nuclear magnetic resonance imaging (NMR) and positron emission tomography (PET) imaging techniques. These are similar, in terms of location and characteristic NMR and PET features, to those that occur in the brain of about 10% of clinical research human subjects, who have been treated for intracranial vascular malformations with stereotactic radiosurgery. These lesions have been described radiologically as "vasogenic edema of the deep white matter", and the injury is of variable intensity and temporal duration, can recede or progress to serious neurologic sequelae, and persist for a considerable period of time, frequently 18 mon to 3 yr.

† Supported by the Office of Health and Environmental Research, U.S. Department of Energy contract DE-AC03-76SF00098.

Our research group is engaged in focal charged particle irradiation of life-threatening vascular disorders of the brain. These congenital vascular abnormalities are composed of a tangle of malformed blood vessels, of which the most common is called "arteriovenous malformation", or AVM for short. These blood vessels can rupture at a rate of approximately 3% to 4% per year and the resulting hemorrhage can cause brain injury leading to neurological problems such as paralysis or blindness, and may even cause death in some instances. Many of these lesions are operable, but in some cases they are located in deep or critical structures that are inaccessible to neurosurgical approaches without a high risk of injury or death. In these cases we have found that focal irradiation with charged particle beams, such as accelerated helium ions, can obliterate over 90% of the targeted volume over a two year period following irradiation. Radiation injury to the target AVM blood vessels will cause endothelial cell damage and abnormal proliferation leading to luminal narrowing, hemostasis, thrombosis, and eventual closure of the AVM. Angiographic obliteration of the AVM during follow-up studies of treated patients can be quite dramatic. Even if complete obliteration of the AVM is not achieved, radiation-induced thickening of the AVM vessel walls can strengthen them and reduce the risks of future hemorrhages.

While we have obtained excellent results, there exists a finite risk of radiation injury to the surrounding brain and normal blood vessels. In some instances this will lead to clinical injury to the patient, the consequences of which can vary from minor to major. One type of radiation injury that we are interested in has been termed "vasogenic edema of the white matter," which shows up on follow-up nuclear magnetic resonance (NMR) and X-ray CT scans as abnormal signals in the deep white matter regions surrounding the previous location of the AVM. NMR imaging has the advantage over CT scanning in this situation because it doesn't use ionizing radiation, so repeated studies may be conducted without excessive X-ray exposure to

the patient. NMR imaging techniques also present better contrast between gray and white matter regions, so a much clearer picture may be obtained of the lesion as it spreads through the white matter tracts in relation to surrounding brain structures. Examples of this phenomenon are shown in the NMR images of two young female patients which are shown in Figures 1 and 2. Figures 1a and 1b are representative axial and coronal plane NMR scans that were taken at 14 mon post-treatment of a left frontoparietal AVM; Figures 1c and 1d are representative scans taken at 36 mon post treatment which shows some degree of resolution and repair of the radiation-induced changes. Figure 2a shows the pre-treatment NMR scan of another young patient with a large left parietal AVM. The AVM appears black on the NMR scan because of the rapid shunting of blood through the lesion. In Figures 2b and 2c we see an initial NMR signal enhancement that is primarily restricted to the immediate white matter regions surrounding the location of the treated AVM. Figures 2b and 2c were taken at 13 mon and 20 mon post-treatment respectively. Figures 2d through 2f were taken at 24 mon, 30 mon, and 34 mon after treatment and show resolution of the white matter injury. The patient in Figure 1 was always clinically normally and never demonstrated any signs of neurologic injury, while the patient in Figure 2 developed a mild right-sided dysfunction and hemiparesis about 20 mon post-treatment which gradually improved in time to the point shown in Figure 2f, where the only sign of a clinical problem was a mild right-foot weakness.

This shows that although NMR scans may present with relatively similar white matter lesions, the clinical outcomes can be very different, thus suggesting that different pathophysiological mechanisms may be possible in this form of delayed radiation injury. What are the temporal sequence of events that lead to the development of these radiation-induced changes? How are some of the changes potentiated by the pretreatment condition of the patient and what are the necessary prerequisites for repair of injury? How does the size and location of the AVM, and

the radiation dose given influence the development of radiation-induced injury and affect the possibility of repair? Can we predict, on the basis of various non-invasive imaging techniques, the clinical outcome of these lesions? These questions serve as our motivation for investigation into the nature of delayed radiation-induced injury and repair in the mammalian brain.

There are a limited number of ways we can approach this problem with humans. X-ray CT scanning can give information on changes that affect the local electron density, such as water density, or contrast agent density when it pools in regions of blood-brain-barrier breakdown. NMR imaging is now preferred over CT scanning for brain studies. The NMR imaging method that we use generally utilizes one of two different pulse-sequence techniques. This is based on the two NMR relaxation times, the spin-lattice relaxation time, T1, and the spin-spin relaxation time, T2. Pathophysiological alterations in brain tissue will lead to changes in the values of these two parameters. Scans which are oriented towards the measurement of T2 are sensitive to the presence of edema and demyelination. Scans which are sensitive to T1 are used in conjunction with the contrast agent, Gadolinium-DPTA (Gd-DTPA), which is sensitive to changes in the blood-brain barrier (BBB). We are also using positron emission tomography (PET) to study brain metabolism, by examining the uptake of ^{19}Fluorodeoxyglucose (^{19}FDG), and to study blood brain barrier breakdown using ^{82}Rubidium (^{82}Rb). Cerebral angiography can show if essential arteries or veins have been occluded. We are studying a number of patients with these techniques. However our high rate of success offers limited access to histologic material. We thus find it difficult or impossible to make fully accurate comparisons and correlations of imaging results with the actual cellular changes occuring in the brain tissues.

In order to better understand the effects of focal irradiation we have found it necessary to develop an animal model. An animal model will not only enable us to

correlate the imaging results with histology, but will allow us to address questions of both scientific and clinical importance. These include effects of different radiations (e.g., photons, helium, carbon, and neon), dose, volume, and fractionation effects, and the possibilities of mitigating some of the effects of radiation injury with various drugs. An animal model will also enable us to test out new imaging strategies that might be potentially useful in our clinical research.

In the initial study, we conducted hemibrain plateau helium ion irradiation of rats. We studied the rats with NMR imaging, but the rat brain proved to be too small to image effectively. The rats died from radiation injury before any lesions could be observed. It became necessary to use a larger animal; three candidates were the rabbit, the cat, or the dog. Since we were primarily interested in effects of delayed radiation injury (edema and BBB alterations) to the central nervous system which are thought to be mediated by vascular and hemodynamic perturbations, we decided to use the rabbit. The rabbit brain is considered to be preferable over the dog or cat brain when studying the cerebral vascular system because cerebral blood supply to the canine and cat brain is delivered primarily through the external carotid arteries with their massive rete mirabile, and the maxillary arteries. In the rabbit brain, cerebral blood supply is not delivered primarily through extracranial anastomoses but is instead balanced very well between the internal carotids and the vertebral system similar to humans, and there is no rete mirabile. The rabbit is also smaller and cheaper and much easier to manage as a laboratory animal compared to the dog so that larger numbers may be used for studies where statistical variations may prove important. We irradiated the left hemisphere of the rabbit brain with a Bragg peak helium ion beam to a depth of only 13 mm, using a hemicircular 20 mm x 10 mm aperture. By stopping the beam at 13 mm, we would spare the deep critical structures of the midbrain from a large radiation dose thus allowing the animals to survive for periods suitable for following the temporal sequence of

changes in the irradiated brain. The irradiations were conducted at the Lawrence Berkeley Laboratory 184-inch Synchrocyclotron. Six rabbits were irradiated to 15 Gy to the left hemibrain, 4 to 30 Gy to the left hemibrain, 2 to 30 Gy to the midline (corpus collosum), and there were 4 controls. From previous experience we expected that radiation-induced changes would develop approximately 8-12 mon after irradiation in the 30 Gy rabbits. It was not completely clear whether the 15 Gy rabbits would develop lesions that would be observable on NMR and PET imaging so these rabbits would serve as a rough measure of the dose response in our model system.

NMR imaging commenced 8 mon after irradiation with a General Electric 1.5 Tesla Magnetic Resonance Imaging system. A human knee coil that fit over the head of the rabbit was used to obtain a good signal to noise ratio; the images had a pixel size of .96 mm.

All rabbits irradiated with 30 Gy to the left hemisphere demonstrated alterations in their functional anatomy as defined by various NMR and PET studies between 8 to 11 mon post-irradiation. T2 weighted NMR scans revealed extensive areas of increased signal in the irradiated hemisphere restricted primarily to the white matter regions (Figure 3a). T1 weighted scans also demonstrated radiation induced changes in the white matter (Figure 3b) but in general these T1 lesions were not as extensive as the T2 lesions. Gd-DTPA NMR images revealed disruption of the BBB indicated by accumulation of the paramagnetic tracer and enhanced signal on the T1 weighted images (Figure 3c). The regions of disrupted BBB were restricted to the deep white matter tracts of the perithalamic area. ^{82}Rb PET scans confirmed the presence of the focal BBB disruptions (Figure 3d). The neuroanatomical location of the ^{82}Rb PET lesions correlated well with the Gd-DTPA NMR images. Although the Gd-DTPA NMR scans appear to be able to define the location and extent of the BBB disruption more clearly, it is unclear if ^{82}Rb

PET may be more sensitive since the Rb ion is much smaller than the Gd-DTPA molecule. ^{18}FDG PET studies demonstrated widespread decrease in ^{18}FDG uptake throughout the cortical regions and associated deep nuclei within the irradiated hemisphere indicating marked metabolic depression (Figure 3e).

Figure 4 shows a series of sequential Gd-DTPA NMR scans that show the slight spreading of the contrast agent from the region of BBB breakdown. It is possible that modifications of this technique might give us some insight into the relative amount of BBB breakdown and the possible dynamics of edema formation. The region of breakdown is at the end of range of the helium beam where the linear energy transfer (LET) of the beam is the highest. The BBB breakdown may occur here as a result of the high LET, or it may be that this region within the deep white matter is particularly sensitive to radiation.

One rabbit irradiated to 30 Gy died from hemorrhage at 10 mon after irradiation. Figure 5a shows a series of NMR scans at 9 mon post-irradiation that show a dark hemorrhagic region within the area of radiation injury. Figure 5b is a photograph of the excised brain and Figure 5c is an NMR image of the excised brain. The right unirradiated side appears normal on the magnetic resonance image, while the left side clearly shows the effects of hemorrhage and edema from radiation injury. We note that the image quality is substantially improved on the excised brain; brain structures are more clearly delineated than on the intact brain of a live rabbit. This is because we are able to image the excised brain with a smaller coil that just fits around the brain, thus improving the signal to noise.

In the two midline 30 Gy rabbits, one died of a respiratory infection before any NMR changes could be seen. In the other midline 30 Gy rabbit we observed BBB breakdown with Gd-DTPA NMR without any clear signs of abnormalities as seen on T2 weighted NMR images (Figures 6a-b). This peculiar phenomenon persists through 14 mon post-irradiation and the rabbit is still clinically fine; it is

unclear if the corpus collosum is more resistant to injury so further experiments are necessary. It is also possible that Gd-DPTA NMR images can be used to detect BBB breakdown that could be an early marker for delayed radiation injury from focal radiation. We will pursue this possibility in our next series of experiments. If confirmed, these results could prove useful in the clinical management of radiation injury in human patients. Some rabbits have been sacrificed and histological studies are being conducted. All the surviving rabbits are being followed closely for any signs of repair of injury especially resolution of edema within the white matter tracts. All 15 Gy rabbits are still normal at 14 mon post-irradiation.

In summary, we have developed an animal model for radiation injury. Lesions are observable using NMR and PET scanning. The rabbits do not deteriorate rapidly upon the appearance of these lesions so that the temporal evolution of the injury may be followed, thus allowing for the possibility of studying repair of radiation injury that has been shown to occur in our clinical human subjects. Eventually histopathological findings will be correlated with the NMR and PET results. We believe that the results of developing this model will prove crucial to the management and followup of human patients who are treated by focal irradiation for various intracranial disorders.

Bibliography

1. W.Calvo, J.W.Hopewell, H.S.Reinhold, T.K.Yeung, Time and dose related changes in the white matter of the rat brain after single doses of X rays. *British J Radiology*, 61, 1043-1052: 1988.

2. E.C.Crosby, H.N.Schnitzlein (eds), Comparative correlative neuroanatomy of the vertebrate telencephalon. MacMillan, New York: 1982.

3. J.I.Fabrikant, J.T.Lyman, K.A.Frankel, Heavy charged particle Bragg peak radiosurgery for intracranial vascular disorders. *Rad Res*, 104, s244-s258: 1985.

4. J.R.Fike, C.E.Cann, K.Turowski, R.J.Higgins, A.S.L.Chan, T.L.Phillips, R.L.Davis, Radiation dose response of normal brain. *Int J Radiation Oncology Biol Phys*, 14, 63-70: 1988.

5. R.I.Grossman, C.M.Hecht-Leavitt, S.M.Evans, R.E.Lenkinski, G.A.Holland, T.J.Van Winkle, J.T.McGrath, W.J.Curran, A.Shetty, P.M.Joseph, Experimental radiation injury: combined MR imaging and spectroscopy. *Radiology*, 169, 305-309: 1988.

6. R.P.Levy, J.I.Fabrikant, K.A.Frankel, M.H.Phillips, J.T.Lyman, Stereotactic heavy charged particle Bragg peak radiosurgery for the treatment of intracranial arteriovenous malformations in childhood and adolescence. *Neurosurgery* (in press.)

7. E.H.Lo, K.A.Frankel, A.Poljak, M.H.Phillips, J.I.Fabrikant, K.H.Woodruff, K.Brennan, R.Delapaz, P.E.Valk, Focal heavy charged particle irradiation of the mammalian cortex : temporal pattern of changes followed by magnetic resonance imaging and positron emission tomography. In conference proceedings, Radiosurgery: a Neurosurgical Approach to Intracranial Disorders, University of Virginia Medical School, 1989.

8. K.H.Woodruff, J.T.Lyman, J.I.Fabrikant, Heavy charged particle induced lesions in rabbit cerebral cortex. *Int J Radiation Oncology Biol Phys*, 14, 301-307: 1988.

Figure Legends

Figure 1 Sequential NMR scans of a 15 year old girl who presented with uncontrolled seizures from a left frontoparietal AVM. A dose of 45 Gy of Helium ions (230 MeV/amu) was delivered stereotactically to the AVM using 5 ports in 2 days to a volume of 3000 mm^3. **a** and **b** show extensive vasogenic edema spreading through the parietal and frontal deep white matter 14 mon after radiosurgery. The patient was, however, free of neurologic symptoms. **c** and **d** show resolution of the injury 36 mon after treatment. Currently the AVM is completely obliterated and the patient enjoys good health.

Figure 2 Sequential NMR scans of a 15 year old girl with a very large left parietal AVM. A dose of 32 Gy of Helium ions was delivered with 4 ports in 2 days to a volume of 26000 mm^3. She developed mild right-sided hemiparesis but improved markedly with corticosteroid therapy and upon subsequent resolution of the white matter injury. The AVM has been completely obliterated and the patient now no longer requires any steroids. **a** shows the AVM before treatment. **b** and **c** shows the abnormal white matter signal spreading at 13 mon and 20 mon post-treatment respectively. **d** and **e** and **f** shows the resolution of injury at 24 mon, 30 mon, and 34 mon after treatment.

Figure 3 Coronal NMR and PET scans of a left hemisphere 30 Gy (helium ions) rabbit at 10 mon after irradiation. Injury is shown to be restricted to the left irradiated hemisphere. **a.** T2 weighted NMR scan demonstrating the abnormal signals restricted primarily to the white matter tracts of the corona radiata and the perithalamic and thalamic regions. **b.** T1 weighted NMR scan shows the region of injury restricted to the deep white matter. **c.** Gd-DTPA NMR scan demonstrates the focal region of BBB disruption in the irradiated hemisphere. **d.** Rb PET scan confirms the presence of the BBB disruption. **e.** coronal FDG PET scan shows the

extensive metabolic depression throughout the left irradiated hemisphere.

Figure 4 A series of Gd-DTPA NMR scans of 30 Gy rabbit that shows the slight spreading of the contrast agent from the central area of BBB disruption. The scans were taken 10, 20, 30, 40 min after infusion of the agent through a ear vein catheter.

Figure 5 A 30 Gy rabbit demonstrated a hemorrhagic lesion within the region of injury 9 mon after irradiation. It died of a second massive hemorrhage 10 mon after irradiation. **a** shows the original T2 weighted NMR scan before death with the dark areas of hemorrhage with associated edema. **b** shows the excised brain with the large hemorrhage that is visible in the left hemisphere. **c.** T2 weighted NMR scan of the excised brain in a smaller proton coil that shows the extent of injury in the irradiated hemisphere with greater resolution and clarity.

Figure 6 A 30 Gy rabbit radiated to the midline shows a unique type of injury 11 mon later. **a.** Regular T2 weighted scans do not reveal any lesions. **b.** However, a Gd-DTPA enhanced NMR scan shows the BBB is severely disrupted in the irradiated corpus collosum.

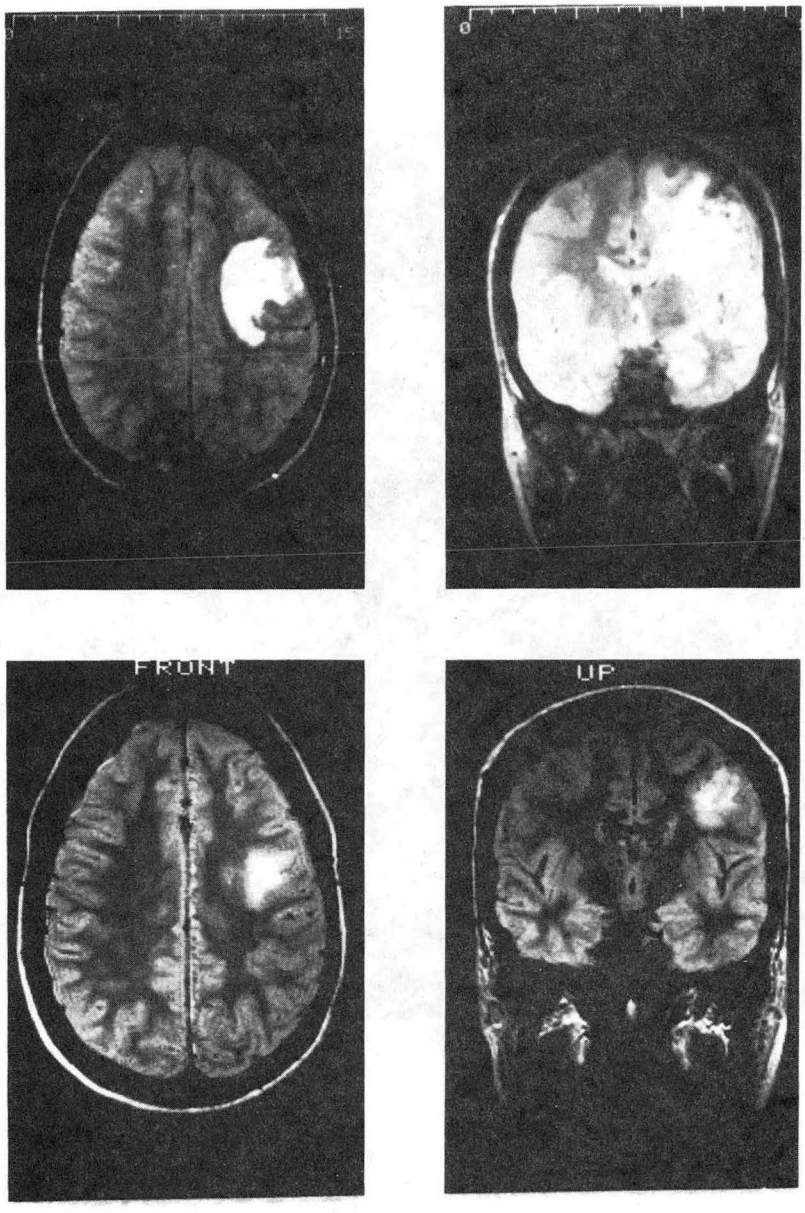

XBB 870-9124

Fig. 1a-d

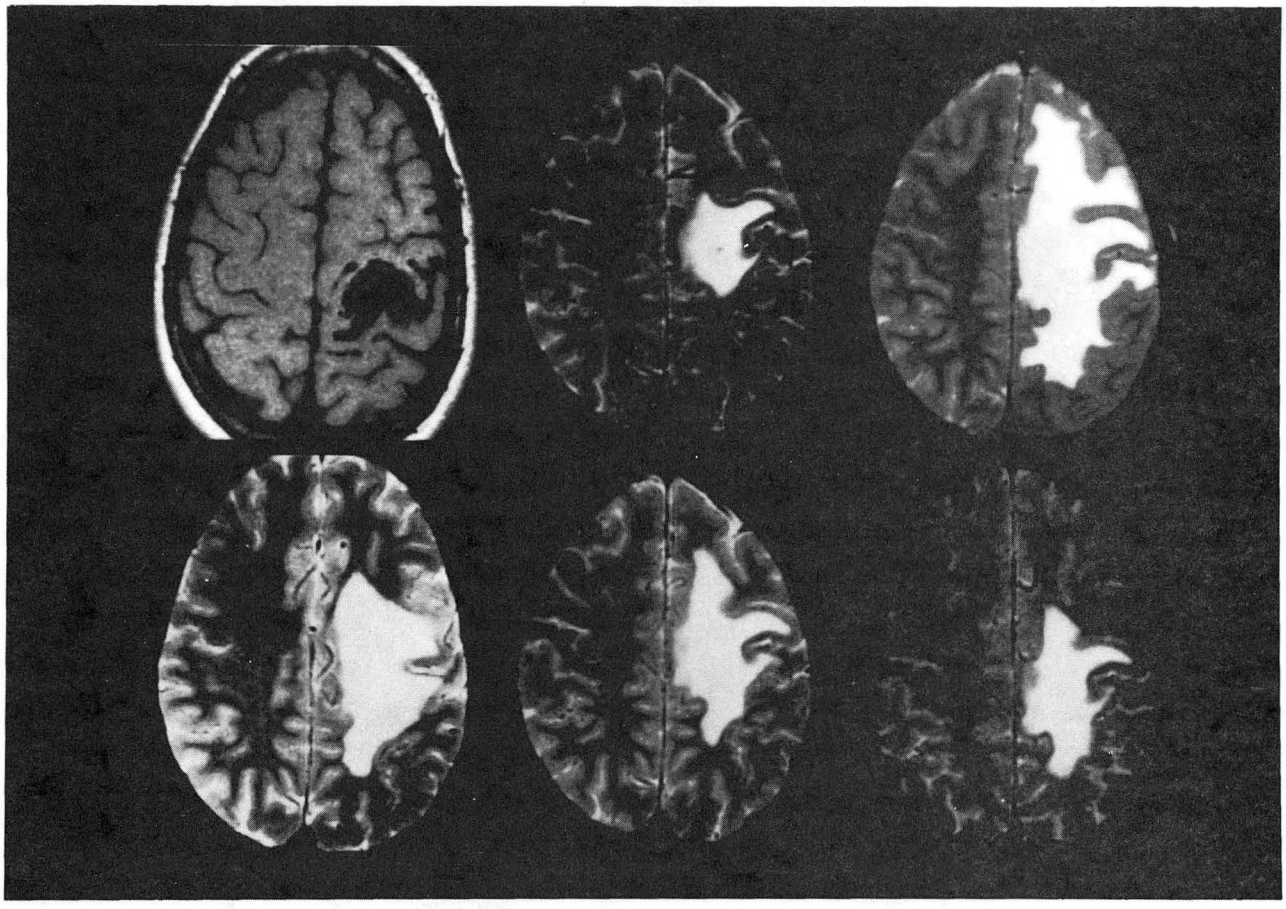

XBB 884-4125

Fig. 2a-f

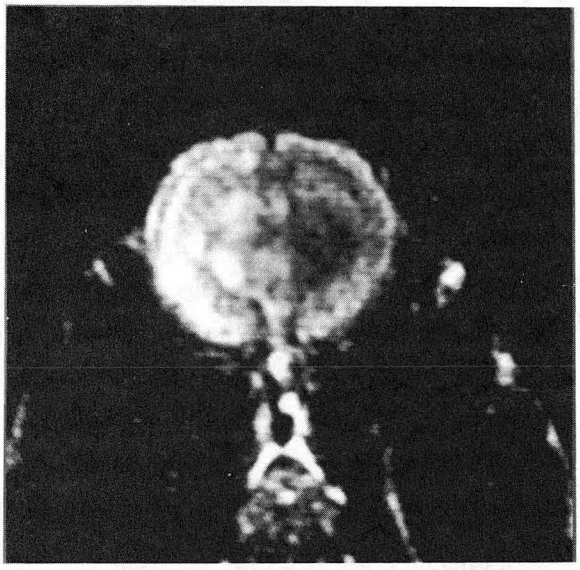

Fig. 3a

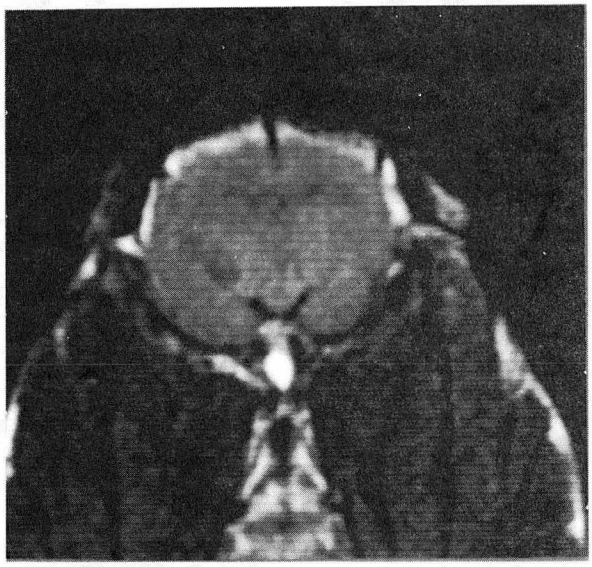

Fig. 3b

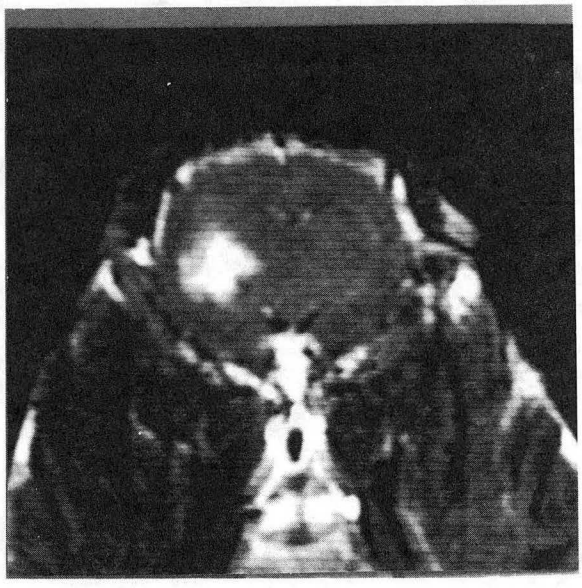

Fig. 3c

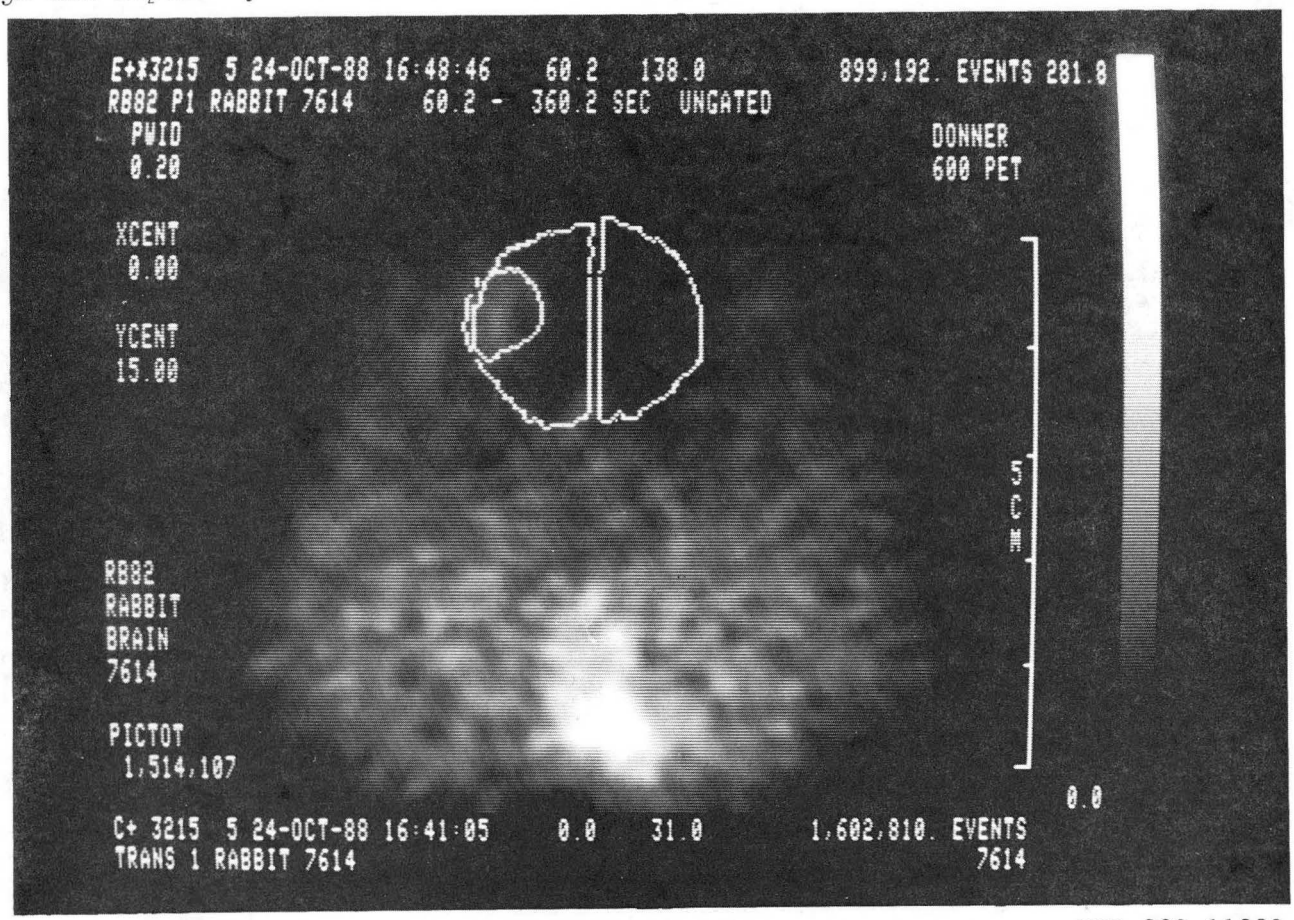

CBB 889-11829

Fig. 3d

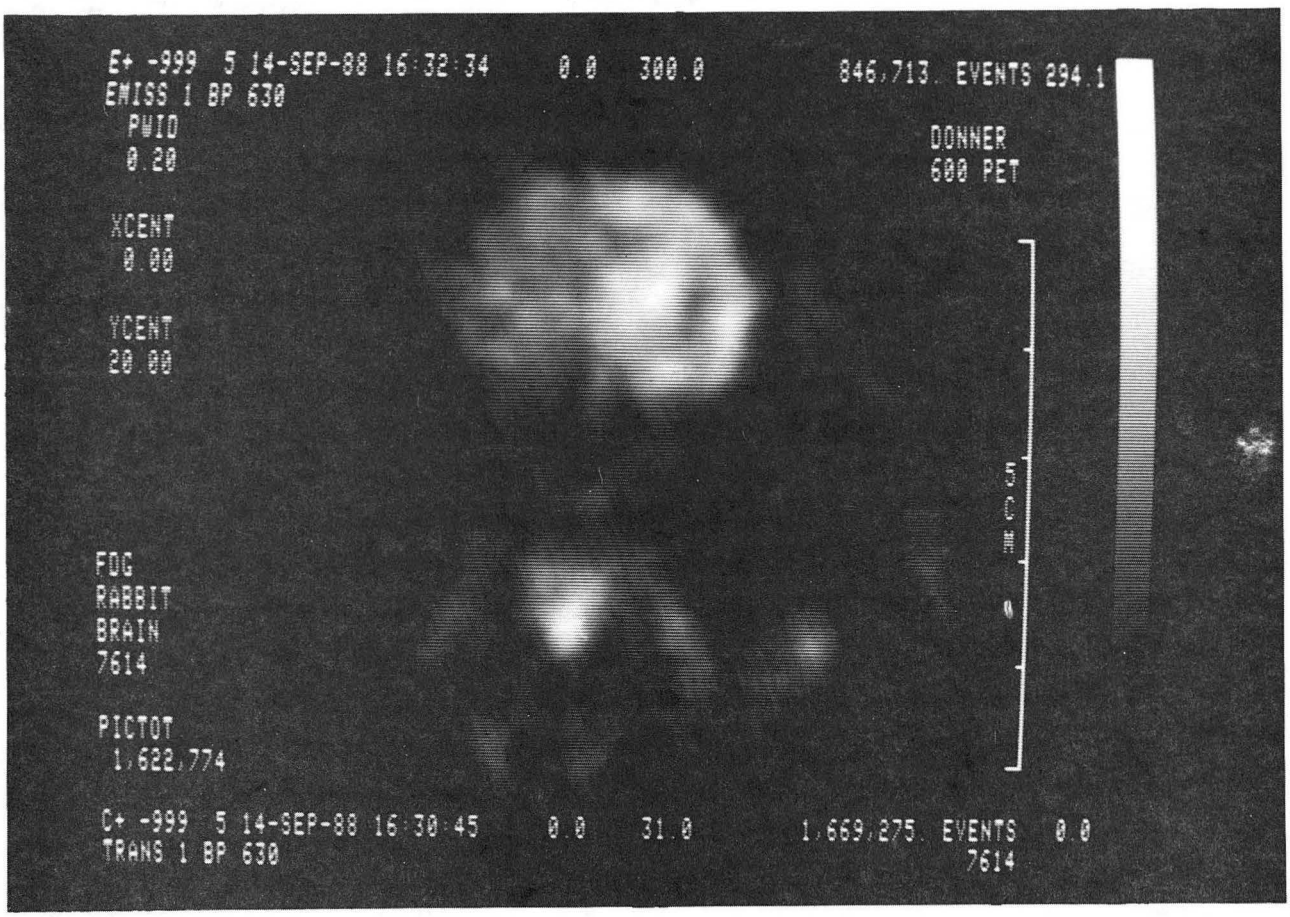

CBB 880-11823

Fig. 3e

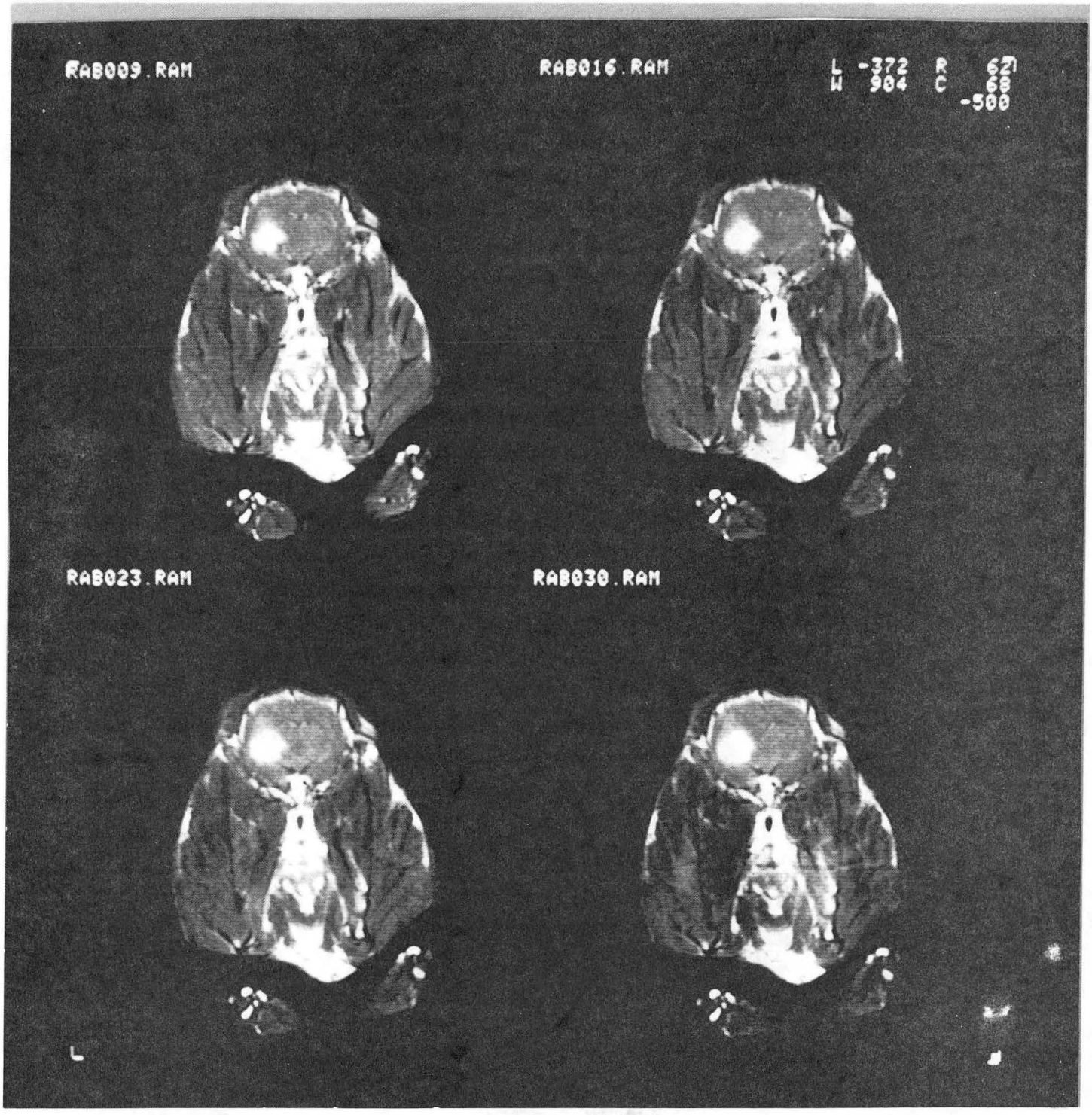

XBB 880-11834

Fig. 4

Fig. 5a

CBB 889-10145

Fig. 5b

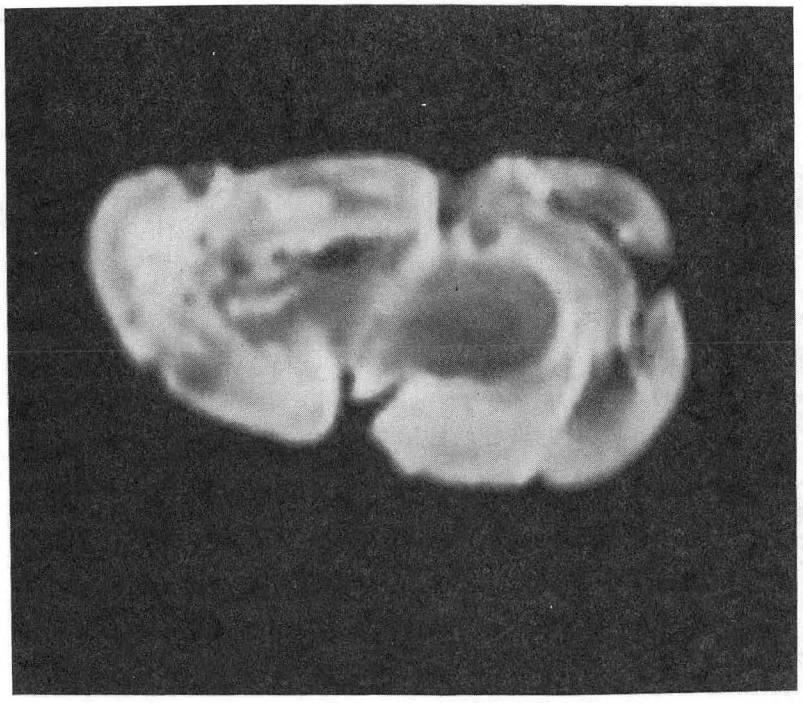

XBB 891-545

Fig. 5c

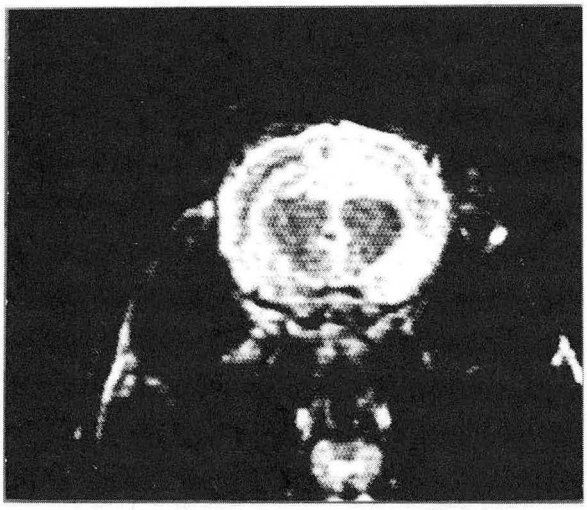

Fig. 6a

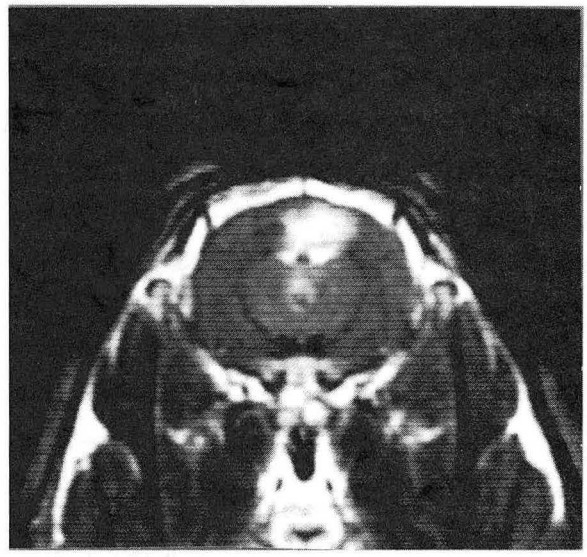

Fig. 6b

LAWRENCE BERKELEY LABORATORY
TECHNICAL INFORMATION DEPARTMENT
1 CYCLOTRON ROAD
BERKELEY, CALIFORNIA 94720